THE JOURNAL OF BIOLOGICAL CHEMISTRY VOL. 283, NO. 42, pp. 28401–28412, October 17, 2008

Regulation of CFTR Trafficking by Its R Domain*[S]

Received for publication, January 22, 2008, and in revised form, June 25, 2008 Published, JBC Papers in Press, August 11, 2008, DOI 10.1074/jbc.M800516200

Christopher M. Lewarchik, Kathryn W. Peters, Juanjuan Qi, and Raymond A. Frizzell[1]

From the Department of Cell Biology and Physiology, University of Pittsburgh School of Medicine, Pittsburgh, Pennsylvania 15261

Phosphorylation of the R domain is required for cystic fibrosis transmembrane conductance regulator (CFTR) channel gating, and cAMP/protein kinase A (PKA) simulation can also elicit insertion of CFTR into the plasma membrane from intracellular compartments (Bertrand, C. A., and Frizzell, R. A. (2003) *Am. J. Physiol.* 285, C1–C18). We evaluated the structural basis of regulated CFTR trafficking by determining agonist-evoked increases in plasma membrane capacitance (C_m) of *Xenopus* oocytes expressing CFTR deletion mutants. Expression of CFTR as a split construct that omitted the R domain (Δamino acids 635–834) produced a channel with elevated basal current (I_m) and no ΔI_m or trafficking response (ΔC_m) upon cAMP/PKA stimulation, indicating that the structure(s) required for regulated CFTR trafficking are contained within the R domain. Additional deletions showed that removal of amino acids 817–838, a 22-amino acid conserved helical region having a net charge of −9, termed NEG2 (Xie, J., Adams, L. M., Zhao, J., Gerken, T. A., Davis, P. B., and Ma, J. (2002) *J. Biol. Chem.* 277, 23019–23027), produced a channel with regulated gating that lacked the agonist-induced increase in CFTR trafficking. Injection of NEG2 peptides into oocytes expressing split ΔNEG2 CFTR prior to stimulation restored the agonist-evoked ΔC_m, consistent with the concept that this sequence mediates the regulated trafficking event. In support of this idea, ΔNEG2 CFTR escaped from the inhibition of wild type CFTR trafficking produced by overexpression of syntaxin 1A. These observations suggest that the NEG2 region at the C terminus of the R domain allows stabilization of CFTR in a regulated intracellular compartment from which it traffics to the plasma membrane in response to cAMP/PKA stimulation.

The cystic fibrosis transmembrane conductance regulator (CFTR)[2] is a phosphorylation-activated anion channel located at the apical membranes of airway, intestinal, pancreatic, and salivary gland epithelial cells. Its stimulation, primarily by cAMP-dependent signaling pathways, is the basis of electrolyte and fluid secretion that provides the fluid vehicle for macromolecular secretory products. In airway epithelia, CFTR is the principal apical anion conductance contributing to chloride and HCO_3 secretion, and this establishes the electrical and osmotic driving forces for secondary sodium and water transport. Together, these events regulate the volume and composition of the airway surface liquid (3, 4). Mutations in the gene encoding CFTR cause cystic fibrosis by either reducing its apical membrane density or interfering with its ability to transport anions (4).

Identification of the primary amino acid sequence (5) placed CFTR in the ATP-binding cassette (ABC) transporter superfamily, of which there are ~50 members in the human genome. Similar to other ABC transporters (6), the N terminus of CFTR leads to six membrane-spanning segments that comprise the first transmembrane domain (TMD1), followed by a nucleotide-binding domain (NBD1). These structural elements are repeated in the C-terminal half of CFTR, as TMD2 and NBD2, followed by a C-terminal tail. A unique feature of CFTR among ABC family members is the presence of a regulatory (R) domain, interposed between these repeated TMD-NBD elements, whose multiple phosphorylation sites mediate cAMP-dependent channel activation by protein kinase A (PKA) (7). The multiple PKA phosphorylation sites of the R domain act in concert to enable gating, and site mutagenesis has not revealed a requirement for phosphorylation at specific loci (8). Rather, there is redundancy in the ability of R domain PKA sites to support channel activation. The unstructured nature of the R domain (9) was confirmed in recent NMR structural studies, which showed that this largely disordered region contains segments of helical structure that likely interact with other CFTR domains, and perhaps other proteins, to effect its regulatory functions (10).

Phosphorylation of the R domain is required for channel gating, which is then driven by the binding and hydrolysis of ATP at the NBDs of CFTR (11–14). The formation of a head-to-tail NBD1/NBD2 dimer is thought to create shared ATP-binding sites that are contributed by residues from both NBDs, an arrangement based on bacterial ABC transporter structures (15). Conversely, the reversal of PKA-mediated channel activation requires R domain dephosphorylation, which is facilitated by phosphatases 2A and 2C (16).

The current view of R domain regulation of channel gating involves both inhibitory and stimulatory properties of this region. Under nonstimulated conditions, channel gating is inhibited by R domain elements that perhaps interfere with

* This work was supported, in whole or in part, by National Institutes of Health Grants DK68196 and DK72506. This work was also supported by the Cystic Fibrosis Foundation. The costs of publication of this article were defrayed in part by the payment of page charges. This article must therefore be hereby marked "*advertisement*" in accordance with 18 U.S.C. Section 1734 solely to indicate this fact.

[S] The on-line version of this article (available at http://www.jbc.org) contains supplemental Figs. 1 and 2.

[1] To whom correspondence should be addressed: Dept. of Cell Biology and Physiology, University of Pittsburgh School of Medicine, S368 BST, 3500 Terrace St., Pittsburgh, PA 15261. Tel.: 412-648-9498; Fax: 412-648-8330; E-mail: frizzell@pitt.edu.

[2] The abbreviations used are: CFTR, cystic fibrosis transmembrane conductance regulator; ENaC, epithelial sodium channel; IBMX, isobutylmethylxanthine; PKA, protein kinase A; WT, wild type; F, farad; HRP, horseradish peroxidase; NBD, nucleotide-binding domain; TMD, transmembrane domain; EXT, extope; HA, hemagglutinin; BFA, brefeldin A; ABC, ATP-binding cassette; sNEG2, scrambled NEG2; hNEG2, helical NEG2.

NBD dimer formation. This model is supported by the finding that addition of the nonphosphorylated R domain to the cytoplasmic face of active CFTR channels is inhibitory (17). Conversely, a stimulatory action of the R domain was implicated by the properties of CFTR channels bearing a large R domain deletion (708–835), which gate with reduced open probability, but are stimulated by the addition of a phosphorylated R region polypeptide (amino acids 645–835) (18). Finally, it appears that the location of the R domain, at the center of the repeated ABC structure, is not critical to channel regulation, because its transplantation to the C terminus of CFTR, together with a sufficient linker region, also conferred regulated CFTR channel function (19).

In addition to regulating channel gating, cAMP agonists also modulate the density of CFTR channels in the plasma membrane in many systems (for review see Ref. 1). Accordingly, the cAMP/PKA-induced increase in anion current associated with phosphorylation-dependent increases in CFTR open probability (P_o) is supported also by an increase in the number of channels (N) resident in the surface membrane. The influence of CFTR on membrane trafficking was first demonstrated in cystic fibrosis pancreatic cells in which the exogenous expression of WT CFTR produced a cAMP-dependent inhibition of endocytosis and stimulated the return of internalized membrane to the cell surface (*i.e.* recycling) (20). Similar results were obtained from human airway cells endogenously expressing WT CFTR, in which cAMP stimulation increased the release of previously internalized fluorescein isothiocyanate-dextran (21). This exocytic event coincided with an increase in membrane capacitance, and these responses were present only in cells expressing WT CFTR. In addition, the kinetics of CFTR trafficking were relatively rapid. Following biotinylation of the cell surface, CFTR was internalized at rates that approached those of endocytic model proteins, such as the transferrin receptor (22, 23).

In *Xenopus* oocytes, the transit of CFTR to the cell surface, detected with an external epitope-tagged CFTR construct, paralleled acute cAMP/PKA-induced increases in membrane current and capacitance, and these functional responses were not observed in the absence of CFTR expression (24, 25). Importantly, CFTR immunolocalization data obtained with native tissues endogenously expressing CFTR provided data consistent with its agonist-evoked trafficking to the apical plasma membrane (26, 27) Thus, biochemical, morphological, and functional evidence of regulated CFTR trafficking has been presented for a number of epithelial and nonepithelial systems (1).

Nevertheless, data conflicting with this concept have emerged as well. Although some negative findings can be attributed to the use of exogenous overexpression systems or nonphysiological experimental conditions (reviewed in Ref. 1), it is evident also that an appropriate cellular background is needed to support regulated CFTR trafficking processes. Context dependence of cellular trafficking events is observed not only for CFTR, but for other channels and transporters (1). Thus, the ability of agonists to alter plasma membrane CFTR density varies among cell types, likely because of variable expression of the required trafficking machinery and interacting proteins. However, the discovery that disease-causing mutations influence plasma membrane CFTR density by affecting its trafficking in distal secretory and recycling compartments (28, 29) highlights the significance of these processes and their contribution to normal epithelial functions. The inability of the common CFTR mutant to recycle to the plasma membrane following its internalization is a significant factor complicating the therapeutic rescue of ΔF508 CFTR to the cell surface (28, 30, 31).

The trafficking pathways and associated protein interactions that underlie regulated CFTR trafficking remain poorly defined. Prior studies have indicated that the CFTR trafficking response is robust in *Xenopus* oocytes expressing WT CFTR, demonstrated by parallel increases in membrane conductance (G_m) and capacitance (C_m) in response to cAMP/PKA stimulation (32). These findings were supported also by increased cell surface detection of CFTR bearing an external epitope tag (25), and increases in plasma membrane CFTR density were detected using atomic force microscopy applied to membranes from oocytes expressing CFTR (33). These findings, together with the unitary relationship between the surface area and the electrical capacitance of biological membranes (1 μF/cm^2), are consistent with the concept that cAMP/PKA stimulation elicits the fusion of CFTR-containing membranes from intracellular compartments with the plasma membrane.

In this study, we examined the structural basis of regulated CFTR trafficking using a series of CFTR deletion constructs, by assessing their cAMP/PKA-induced membrane current and capacitance responses. Our goal was to determine whether there are regions of CFTR required for its regulated trafficking. In addition to producing a nonregulated chloride current in the absence of stimulation, we found that removal of the R domain eliminated the cAMP/PKA-induced membrane capacitance increase. Further structure-function analysis of R domain deletion constructs showed that removal of its C-terminal region produced a channel that retained agonist-dependent current regulation, but eliminated its cAMP/PKA-mediated trafficking, as reflected by the agonist-induced increase in C_m. These findings suggest that a small, ordered R domain segment can stabilize CFTR within intracellular compartments, whereas R domain phosphorylation, by interfering with this intracellular stabilization, permits the redistribution of CFTR to the cell surface.

EXPERIMENTAL PROCEDURES

Constructs and Antibodies—CFTR deletion constructs were generated via PCR using *PFU* polymerase (Invitrogen) according to the manufacturer's instructions. PCR-generated deletion constructs were subcloned into pcDNA3.1 using the pcDNA3.1/V5-His TOPO® TA expression kit (Invitrogen) according to instructions. All constructs were sequenced to verify fidelity. Site-directed mutagenesis of residues in the R domain to generate hNEG2-CFTR or sNEG2-CFTR was performed using the GeneTailor™ site-directed mutagenesis system from Invitrogen. For these large modifications, regions were mutated sequentially, with the previously mutated region serving as the template for subsequent mutagenesis reactions. Following the production of each mutation, the entire template was sequenced.

Oocyte Preparation—Isolation and cRNA injection of oocytes were performed as described previously (34). In short, *Xenopus laevis* females were purchased from *Xenopus* I (Ann Arbor, MI). Surgically isolated oocytes were separated from follicular cells by incubation in 3 mg/ml collagenase (Invitrogen) in calcium-free ND-96 solution at room temperature for 60–90 min followed by devascularization by bathing in 250 mM KH_2PO_4. Following incubation, stage 5 and 6 oocytes were isolated under a dissecting microscope. The oocytes were allowed to recover overnight in modified Barth's solution (mM) as follows: 88 NaCl, 1 KCl, 2.4 $NaHCO_3$, 0.82 $MgSO_4$, 0.33 $Ca(NO_3)\cdot 4H_2O$, 0.41 $CaCl_2\cdot 2H_2O$, 10 HEPES, ½ sodium salt, pH 7.2, with 50 ml of horse serum (Invitrogen) and 0.273 g of sodium pyruvate (Sigma) per liter. The next day, oocytes were injected with 0.5–10 ng of CFTR cRNA (see figure legends). Approximately 25 oocytes were injected with cRNA for each experimental condition, and they were maintained in MBS at 18 °C for 2–3 days prior to current recordings. cRNA was generated using the mMessage mMachine kit (Ambion) for *in vitro* translation of linearized plasmids. Oocytes were co-injected with cRNA encoding the β_2-adrenergic receptor, and stimulation was evoked by addition of 10 μM isoproterenol to the bath.

Electrophysiology—Two electrode voltage clamp recordings employed ND-96 as the bath solution (mM) as follows: 96 NaCl, 1 KCl, 1.2 $CaCl_2$, 5.8 $MgCl_2$, 10 HEPES, pH 7.2. Oocytes were impaled with two glass electrodes filled with 3 M KCl; their resistances were 0.2–1.0 megohms. The electrodes were connected to a GeneClamp 500 current/voltage clamp amplifier (Molecular Devices) via Ag-AgCl pellet electrodes and referenced to Ag-AgCl pellet electrodes in the bath. The oocytes were impaled, and the membrane potentials were allowed to stabilize for ~5 min. The voltage clamp was controlled by an AD/DA interface (AXOLAB 1100), and waveforms were imposed using PC-based software generated in the laboratory.

Membrane capacitance (C_m) was calculated on line from the following relation: $C_m = \tau((1/R_a) + G_m)$, where R_a is the access resistance between the current electrode and the oocyte; G_m is the membrane conductance, and τ is the time constant. A 10-mV hyperpolarizing voltage pulse (50 ms duration) was applied to the holding potential of −30 mV to determine R_a, G_m, and τ. As illustrated in Fig. 1*A*, τ was obtained by fitting the exponential current decay curve during the voltage pulse; in this interval, the current sampling rate was 170 kHz and permitted the acquisition of 1700 data points in 10 ms. R_a was calculated from V_p/I_{pp}, where I_{pp} is the instantaneous current obtained from extrapolation of the experimental fit to zero time. The peak of current was detected, and 250 points following the peak were fit using a first-order exponential decay function, indicated as the *red overlay* in Fig. 1. The steady-state current, I_{ss}, was used to calculate G_m from the average of three points taken near the end of the pulse, using the relation $(I_{ss}/(V_p - R_a \times I_{ss}))$. This approach provides a reliable estimate of C_m both before and after the rather large change in membrane conductance associated with cAMP/PKA stimulation in CFTR expressing oocytes. In the repetitive pulse protocol, V_m was held at −30 mV, approximating the chloride equilibrium potential, and pulsed to −40 mV (50 ms) to obtain C_m, as described. V_m was returned to −30 mV (100 ms) and then pulsed to −60 mV (200 ms) to obtain the reported transmembrane current, I_m, which was sampled 10 ms before the end of each pulse. This protocol was repeated every 5 s throughout the experiment.

Co-injection of NEG2 Peptides—The NEG2 peptide, derived from the C terminus of the R domain, and two modified peptides (sNEG2 and hNEG2), see figure legends for definition, were synthesized via solid-phase peptide synthesis, kindly provided by Dr. Robert Bridges (Rosalind Franklin University). Each peptide was solubilized at a concentration of 50 μM in an intracellular buffer (35) containing (mM) the following: 128 potassium glutamate, 5 NaCl, 7 $MgSO_4$, 20 HEPES, pH 7.0, titrated with ultrapure KOH, aliquoted, and stored at −20 °C. Oocytes expressing ΔNEG2-CFTR were voltage-clamped as described above and allowed to equilibrate for 5 min. NEG2, or a modified peptide, was drawn into an injection tip similar to that used for cRNA injections; the clamp was interrupted, and oocytes were impaled and injected with 23 nl of NEG2 peptide solution. Twenty minutes following peptide injection, experimental recordings were initiated using the standard agonist addition and recording protocols described above.

Immunoblots and Cell Surface Labeling—Western blotting of *Xenopus* oocyte extracts was performed as described (36). Briefly, oocytes were homogenized in 15 mM Tris, pH 6.8, in 20 μl of buffer/oocyte. An equal volume of 1,1,2-trichloro-trifluorethane (Freon) was added, and the oocytes were spun for 10 min at maximum speed in a bench top centrifuge. The upper phase was recovered, and the remainder was treated again with Freon. Proteins were precipitated with ice-cold methanol and chloroform. Sample buffer was added; the proteins were separated by SDS-PAGE and transferred to Immobilon™-P. Blots were probed with R domain-specific α-hCFTR mouse monoclonal IgG (1:1000) from R & D Systems (Minneapolis, MN) or the mouse monoclonal antibody (1:2500) whose epitope lies at the CFTR C terminus (clone 24-1), which was purified from hybridoma supernatant (HB-11947; ATCC) by Mark Silvis in the laboratory. The secondary antibody was donkey α-mouse horseradish peroxidase (HRP) from Amersham Biosciences (1:5000).

Labeling of CFTR at the cell surface utilized an externally epitope-tagged CFTR construct (EXT-CFTR (37)), kindly provided by Dr. John Riordan (University of North Carolina, Chapel Hill). HEK 293 cells were transiently transfected with cDNA constructs encoding EXT-CFTR or WT CFTR (control), 4 μg/35-mm dish, 24 h prior to experiments using Lipofectamine 2000 (Invitrogen) according to the manufacturer's instructions. Following transfection, cells were incubated in HEK 293 media (Dulbecco's modified Eagle's medium + 10% fetal bovine serum) at 37 °C overnight. Cells were stimulated with 10 mM forskolin (EMD Biosciences) at 37 °C for 12 min and placed on ice. For oocyte studies, EXT-CFTR (10 ng) or WT CFTR (1 ng) cRNA was injected together with β-adrenergic receptor and incubated in MBS^{++} for 3 days at 18 °C. Oocytes were stimulated with 10 μM isoproterenol (Sigma) as in the electrophysiological studies. Nonstimulated HEK cells or oocytes, treated identically except for agonist additions, served as controls. For chemiluminescence measurements, cell surface EXT-CFTR was labeled by sequential incubations in primary

monoclonal HA antibody (1:1000, 90 min) (Covance, New York), secondary biotin-conjugated goat anti-mouse IgG (1:200, 90 min) (Invitrogen), and streptavidin conjugated to HRP (1:500; 90 min) (Zymed Laboratories Inc.). All steps were performed at 4 °C to block CFTR trafficking. The cells were then washed extensively, and HRP-labeled proteins were detected using SuperSignal West Femto chemiluminescent substrate (Pierce) and read in a TD20/20 luminometer (Turner, Sunnyvale, CA).

Statistics—All data are presented as means ± S.E., where N indicates the number of experiments, and n is the total number of oocytes studied. Statistical analysis was performed using the Student's unpaired t test. A value of $p \leq 0.05$ is considered statistically significant, as indicated (by *) in all figures. All experiments were performed on oocytes harvested from at least three *X. laevis* to judge reproducibility. The functional half-life of different CFTR constructs was determined by fitting current decay curves obtained in the presence of brefeldin A with the two-parameter, single exponential decay regression function of SigmaPlot 2001 (SPSS, Chicago).

Calculations—We calculated the number of vesicles (N_v) inserted into the plasma membrane in response to cAMP/PKA stimulation as described by Bertrand *et al.* (1), using the equation $N_v = \Delta C_m / C_s \cdot 4\pi r_G^2$, where ΔC_m is the measured increase in membrane capacitance; C_s is the specific capacitance of biological membranes (1 μF/cm^2), and r_G is the radius of a spherical vesicle, assumed to be 100 nm for this purpose.

RESULTS

β-Agonist-induced Current and Capacitance Responses—Representative I_m and C_m responses from oocytes expressing WT CFTR are illustrated in Fig. 1, *A* and *B*, and mean data for basal and peak stimulation values from 15 recordings are summarized in Fig. 1*C*. In prior experiments of this type, stimulation was produced by addition of forskolin plus IBMX (24, 25). In this study, co-expression of the β_2-adrenergic receptor allowed cAMP/PKA stimulation by addition of isoproterenol (10 μM) as employed in previous oocyte studies (38, 39). This approach obviates any contribution from the direct interaction of IBMX with CFTR (40) and was used throughout.

Prior to stimulation of oocytes co-expressing CFTR and β_2-adrenergic receptor, basal chloride current was 0.10 ± 0.01 μA, and isoproterenol addition elicited a current increase (ΔI_m) that averaged 2.5 ± 0.13 μA). This current stimulation was paralleled by a 24% increase in membrane capacitance, ΔC_m = 46 ± 9.4 nF, from 192 to 238 nF. These changes in I_m and C_m are CFTR-dependent; they are not observed in uninjected oocytes (not shown) or in oocytes expressing β_2-adrenergic receptor alone (Fig. 3*C*). The magnitudes of these responses are consistent with previously published data obtained using forskolin plus IBMX as the cAMP/PKA agonists (1, 24, 32). In addition, the stimulated current was inhibited 74 ± 4% by the addition of $CFTR_{inh}$-172 (10 μM), which had no significant effect on C_m (data not shown, $n = 5$).

The observed increases in membrane capacitance have been linked to the augmented delivery of CFTR to the plasma membrane, detected in prior studies by immunofluorescence labeling of CFTR bearing a FLAG epitope in its fourth extracellular loop (25). Based on the relationship between biological membrane capacitance and membrane area (1 μF/cm^2), the corresponding increase in plasma membrane area predicted by this capacitance change corresponds to the net fusion of 3.6×10^7 vesicles of 100 nm diameter with the plasma membrane. From the measured ΔI_m, the single channel current of CFTR at the holding voltage (based on single channel conductance of CFTR), and a P_o of 0.4, we predict that a number of channels approximately equivalent to the calculated number of vesicles contributed to the measured current. Therefore, within the limitations of these assumptions, CFTR trafficking to the cell surface appears to account for most of the current response observed in this system, as suggested previously (24).

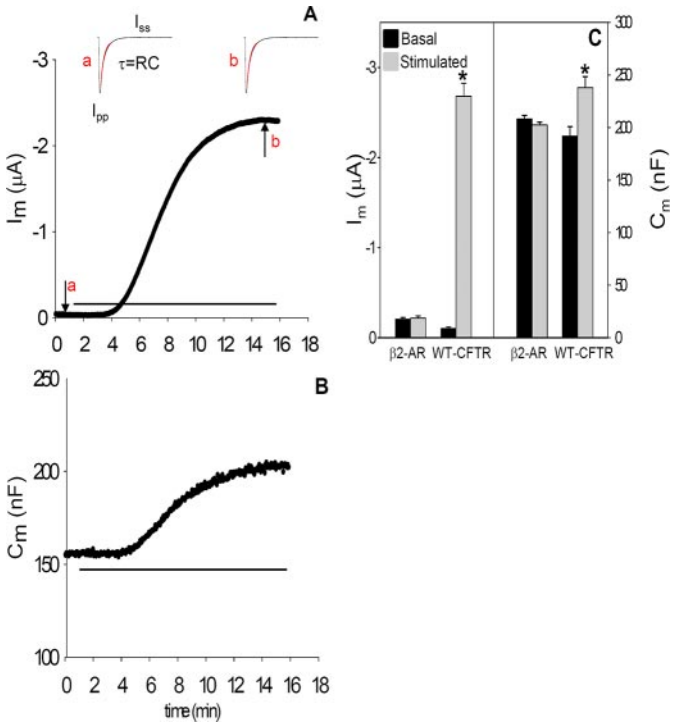

FIGURE 1. I_m (*A*) and C_m (*B*) recordings from a WT CFTR expressing oocyte during stimulation by bath addition of isoproterenol (10 μM), see *horizontal lines*. V_m was held at −30 mV, and I_m was obtained during a 200-mS pulse to −60 mV. C_m was calculated from currents recorded during a 10-mV hyperpolarizing voltage pulse, and *panels a* and *b* of *A* provide current recordings obtained from pulses before and after isoproterenol stimulation at the times indicated in the current record. The *red lines* show the fit of the current transient used to obtain C_m as described under "Experimental Procedures," where I_{ss} is the steady-state current, and I_{pp} is the peak point of the current transient. Each oocyte was injected with 1 ng of WT CFTR plus 1 ng of β_2-adrenergic receptor cRNAs in 50 nl of water. *C,* average basal and stimulated I_m and C_m values are from β_2-adrenergic receptor (*β2-AR*)-injected oocytes ($N = 3$; $n = 10$) or oocytes expressing WT CFTR plus β_2-adrenergic receptor ($N = 4$; $n = 15$). A value of $p < 0.05$ is considered statistically significant and is shown by an *asterisk* in all experiments.

Stimulation Increases the Cell Surface Expression of Extope CFTR—Next, we determined cell surface CFTR expression using a different epitope-tagged CFTR construct and examined the response to β-agonist stimulation. EXT-CFTR contains a hemagglutinin (HA) tag in an expanded second extracellular loop of CFTR (37). It was kindly provided by Dr. John R. Riordan (University of North Carolina, Chapel Hill) and subcloned into pCDNA3.1$^-$, the construct employed to generate other cRNAs. Functional expression of EXT-CFTR exhibited behavior similar to WT CFTR but required ~10-fold more CFTR

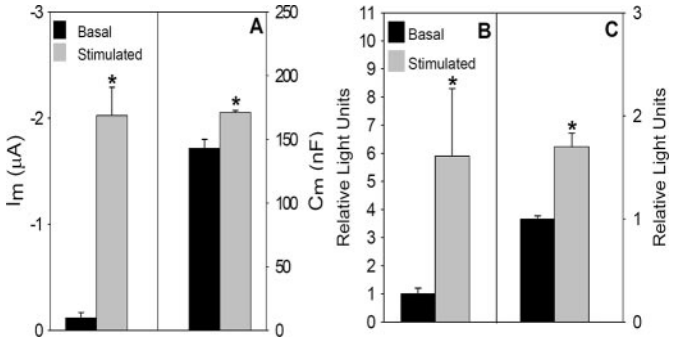

FIGURE 2. **Current, capacitance, and cell surface expression of EXT-CFTR are increased by cAMP/PKA stimulation.** *A*, I_m and C_m were obtained from *Xenopus* oocytes injected with 10 ng of EXT-CFTR and 1 ng of β_2-adrenergic receptor cRNA 3 days prior to measurements ($n = 4$; $n = 17$). Mean luminometry values from oocytes (*B*) or HEK 293 cells (*C*) expressing EXT-CFTR (10 ng of cRNA or 4 μg of cDNA/35-mm plate, respectively) are shown. Values were background-subtracted and normalized to mean values obtained under basal, nonstimulated conditions (oocytes, $N = 4$ and $n = 20$; HEK cells, $N = 5$ and $n = 20$).

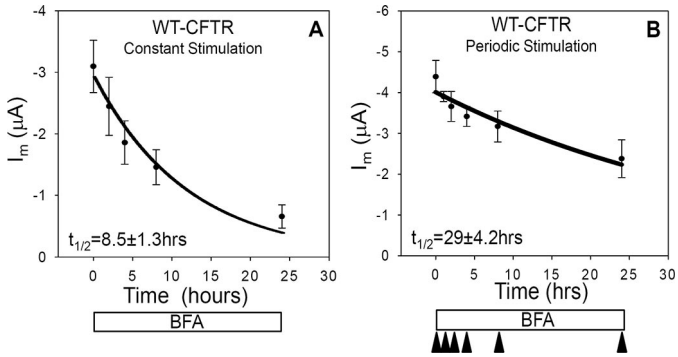

FIGURE 3. **The functional half-life of CFTR is reduced during cAMP/PKA stimulation.** Current decay curves were produced by continuous incubation of oocytes expressing WT-CFTR (1 ng) and β_2-adrenergic receptor (1 ng) with brefeldin A (10 μM). The data were fit with a single exponential function using SigmaPlot (Systat Software). *A*, oocytes were stimulated continuously with 10 μM isoproterenol, and currents were recorded at 0, 2, 4, 8, and 24 h ($N = 5$; $n = 20$, each data point). *B*, currents were recorded from oocytes at separate time points (0, 1, 2, 4, 8, and 24 h) after initial treatment with 10 μM BFA. Current measurements were obtained at maximal stimulation following isoproterenol stimulation at the indicated times by *arrowheads* ($N = 4$; $n = 16$).

cRNA (10 ng/oocyte) to obtain quantitatively similar stimulated current levels. As for WT CFTR, basal chloride currents were low, and addition of isoproterenol increased I_m and C_m ($\Delta I_m = 1.9 \pm 0.21$ μA, $\Delta C_m = 26 \pm 4.1$ nF) (Fig. 2*A*). These values were similar to those obtained from injection of 1 ng of WT CFTR (Fig. 1). The reduced expression efficiency of EXT-CFTR could reflect less effective processing of the protein within the endoplasmic reticulum.

We next used the EXT-CFTR construct to evaluate the influence of cAMP/PKA stimulation on its surface expression by enzyme-linked immunolabeling and luminometry, as described under "Experimental Procedures." Similar experiments were performed in both oocytes and HEK 293 cells. The measurements employed modifications of the protocols described previously (41, 42) in which cells or oocytes were incubated with primary α-HA followed by an α-mouse biotin-conjugated secondary antibody and finally with a streptavidin HRP-conjugated tertiary antibody. This sandwich procedure increased the signal relative to data obtained from a two-antibody protocol (*i.e.* α-mouse-HRP as secondary; data not shown). As shown in Fig. 2, *B* and *C*, cAMP/PKA stimulation produced significant 6- and 2-fold increases in cell surface EXT-CFTR detection in oocytes and HEK cells, respectively. Taken together with the agonist-dependent increases in C_m, the β-agonist-induced surface labeling of EXT-CFTR supports the concept that cAMP/PKA stimulation increases CFTR density in the plasma membrane via fusion of CFTR containing vesicles that are derived from intracellular compartments. The response in oocytes was more robust than that found in HEK cells. In relation to prior studies (25), these data also indicate that the trafficking response does not depend on the position of the epitope tag in CFTR.

Stimulation of CFTR Reduces Its Functional Half-life—Next, we evaluated the hypothesis that the stimulation of CFTR trafficking may alter its functional stability in the plasma membrane. Results consistent with this interpretation have emerged from prior studies of other transporters/channels whose trafficking is subject to acute regulation (43, 44). To examine this possibility, we determined the decay of CFTR currents following the inhibition of anterograde membrane traffic with brefeldin A (BFA), both before and during isoproterenol stimulation of channel trafficking to the cell surface. This method is used commonly to examine the functional half-life of channels in this expression system (45).

As shown in Fig. 3, oocytes expressing WT CFTR were bathed continuously in 10 μM BFA. One group was exposed to continuous stimulation, with agonist present throughout the indicated time course (Fig. 3*A*). The other group was stimulated periodically at the indicated times (*arrowheads*, Fig. 3*B*). When the cells were continuously exposed to agonist, their currents declined more rapidly ($t_{1/2} = 8.5$ h) than those stimulated only at the indicated measurement times ($t_{1/2} = 29$ h). The more rapid decline in current with constant stimulation was not because of β_2-adrenergic receptor desensitization, because similar data were obtained also in response to stimulation by forskolin plus IBMX (data not shown). The decrease in functional channel half-life observed with constant stimulation is consistent with the hypothesis that CFTR is relatively stable when it resides within intracellular compartments prior to stimulation, but that in response to agonist the channel traffics more rapidly through plasma membrane-endosomal pathways, resulting in reduced functional stability. Similar findings have been obtained for GLUT4 and ENaC. In response to insulin, the half-life of GLUT4 was reduced from 50 to 15 h (44), whereas that of ENaC was decreased from 20 to 5 h in response to cAMP stimulation (43). Similarly, the functional half-life of CFTR was reduced by a factor of ~3.5 during continuous cAMP/PKA stimulation.

R Domainless CFTR Lacks Membrane Current and Capacitance Stimulation—Prior studies by Csanady *et al.* (46) have shown that regulated CFTR channel activity could be expressed from half-channels encoded by two cRNA constructs (so-called split CFTR). In preparation for the expression of split CFTR lacking the R domain, we first examined the agonist-evoked changes in current and capacitance of split CFTR expressed from two co-injected cRNAs. Table 1, part A, provides a schematic of the various split CFTR constructs whose properties are

TABLE 1
Summary data for split CFTR constructs

A

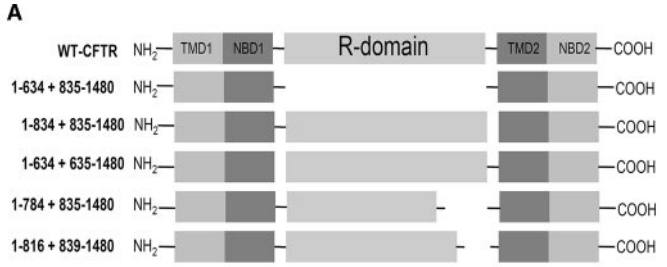

B

cRNA	Basal I_m (μA)	Stimulated I_m (μA)	ng cRNA	n
WT-CFTR	-0.10±0.01	-2.7±0.14	1	15
1-634	-0.10±0.04	-0.02±0.002	0.5	8
835-1480	-0.09±0.02	-0.04±0.01	0.5	10
1-834	-0.16±0.02	-0.02±0.03	0.5	8
635-1480	-0.20±0.04	-0.20±0.02	0.5	9

C

cRNA	Basal I_m (μA)	Stimulated I_m (μA)	ng cRNA	n
1-634 + 835-1480	-1.9±0.17	-2.1±0.18	0.5	29
1-653 + 835-1480	-0.07±0.04	-0.11±0.02	5	7
1-673 + 835-1480	-0.17±0.01	-0.15±0.04	5	8
1-693 + 835-1480	-0.11±0.03	-0.10±0.02	5	7
1-713 + 835-1480	-0.09±0.06	-0.11±0.04	5	10
1-733 + 835-1480	-0.12±0.05	-0.11±0.01	5	8
1-753 + 835-1480	-0.06±0.02	-0.08±0.05	5	11
1-773 + 835-1480	-0.12±0.01	-0.11±0.03	5	7
1-784 + 835-1480	-0.33±0.02	-1.52±0.30	3.5	11
1-816 + 839-1480	-0.84±0.25	-1.9±0.51	3.5	14

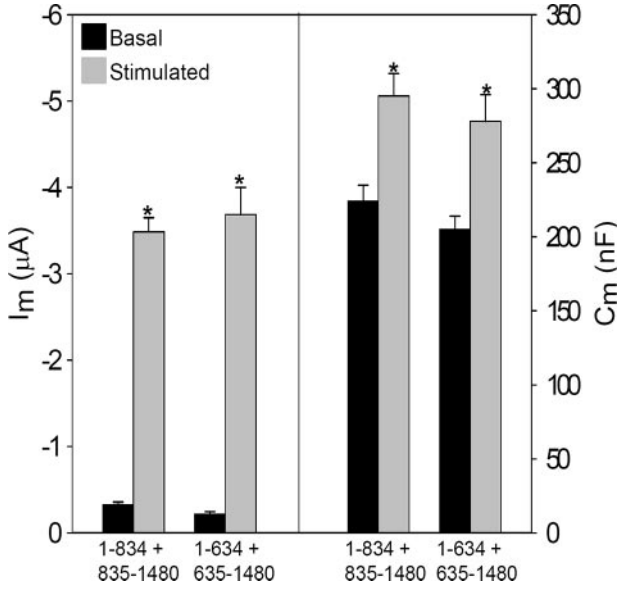

FIGURE 4. **The functional properties of split CFTR constructs resemble those of WT CFTR.** Oocytes were co-injected with 0.5 ng of the CFTR half-channel cRNAs (1–834 + 835–1480 ($N = 4$; $n = 16$) or 1–634 + 635–1480 ($N = 3$; $n = 10$) and 1 ng of β_2-adrenergic receptor, and I_m and C_m were recorded in response to 10 μM isoproterenol, as in Fig. 1.

reported here. The R domain containing constructs encoded amino acids 1–834 or 635–1480, and they were co-expressed with the remaining CFTR sequence from a separate co-injected cRNA, *i.e.* 1–834 + 835–1480 or 1–634 + 635–1480. Fig. 4*A* shows that these split CFTRs, at a similar cRNA dose, behaved indistinguishably from the intact protein (compare with Fig. 1), having low basal currents and substantial increases in both I_m and C_m in response to cAMP/PKA stimulation. The current data replicate those of Csanady *et al.* (46), but the increased C_m values show also that the regulated CFTR trafficking properties of the intact protein are retained. In addition, the functional half-life of split CFTR (1–834 + 835–1480) was similar to that of WT CFTR during constant stimulation (supplemental Fig. 1*A*). Thus, the regulated gating and trafficking properties of WT CFTR are retained in these split constructs, permitting their further modification.

The expression of split CFTR lacking the R domain (1–634 + 835–1480; termed ΔR-N/C) resulted in a high basal current that was not further augmented by cAMP stimulation, as found in previous studies of this construct (46). Fig. 5, *A–C,* shows representative current and capacitance recordings and summary data from oocytes expressing ΔR-N/C CFTR. The spontaneous basal currents produced by omission of the R domain (1.9 ± 0.18 μF) were similar to the stimulated currents of WT CFTR (2.5 ± 0.13 μA) and EXT-CFTR (1.9 ± 0.21). In addition to the absence of an isoproterenol-induced current, stimulation of oocytes expressing ΔR-N/C CFTR did not elicit an increase in C_m (Fig. 5, *B* and *C*). Thus, in addition to forming a constitutively active channel, ΔR-N/C CFTR does not undergo a regulated trafficking response; rather, CFTR lacking its R domain traffics constitutively to the plasma membrane. Also, ΔR-N/C CFTR displayed a relatively short functional half-life (treatment with BFA as in Fig. 3; supplemental Fig. 1*B*), fitting with the idea that it fails to stabilize within intracellular compartments. Together, these findings suggest that the presence of a non-phosphorylated R domain is necessary for CFTR to enter a regulated intracellular compartment from which it is trafficked to the plasma membrane in response to R domain phosphorylation.

In prior studies, we found that the ΔC_m response of WT CFTR reached a plateau as CFTR expression and the corresponding ΔI_m was increased, which was done by augmenting the cRNA dose (24). To verify that the lack of a ΔC_m for ΔR-N/C was not compromised in some way by assessing only a restricted expression level, we determined its ΔC_m-ΔI_m relation over a range of cRNA expression, in comparison with WT CFTR. As supplemental Fig. 2 shows, the ΔC_m response of ΔR-N/C to stimulation was minimal over a broad range of expression. In addition, these data show that the expression level of WT CFTR used in these studies (yielding ~2 μA current) was within the range where ΔC_m is directly proportional to the ΔI_m response.

Individual Half-channel Constructs Do Not Form a Functional Channel—Next, we addressed the possibility that the properties of ΔR-N/C might have arisen from the function of individual half-channels rather than association of the channel halves. Previous studies by Devidas *et al.* (47) suggested that CFTR half-channel constructs composed of TM1 + NBD1 or TM2 + NBD2 formed constitutively active channels when expressed in *Xenopus* oocytes. In view of the high level of cRNA used in those studies (50 ng/oocyte), we asked whether the half-channel constructs would generate significant currents at the lower cRNA levels employed

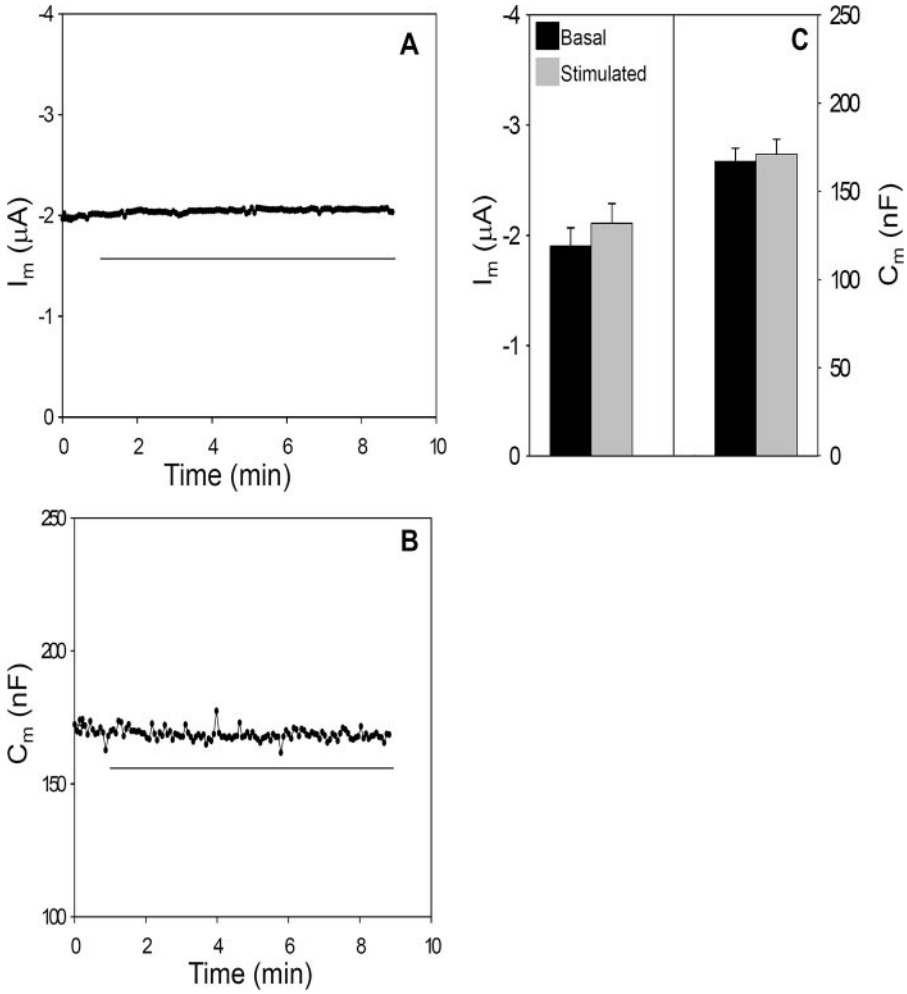

FIGURE 5. **CFTR lacking the R domain does not exhibit regulated current or capacitance responses.** *A* and *B*, time courses of I_m and C_m in an oocyte injected with ΔR-N/C cRNAs (0.5 ng each, 1–634 + 835–1480) plus 1 ng of β_2-adrenergic receptor. *Horizontal line* indicates addition of 10 μM isoproterenol. *C*, summary I_m and C_m data for ΔR-N/C expressing oocytes ($N = 6$; $n = 29$).

here (*i.e.* 0.5 ng/oocyte). Expression was allowed to proceed for the same time period (3 days). The basal and stimulated currents obtained from these cRNAs are provided in Table 1, part B. Relative to WT CFTR, split CFTR, or ΔR-N/C, the individual half-channels did not produce significant currents. Therefore, the currents obtained from split and ΔR-N/C CFTRs derive from assembly of the half-channels.

Expression of the R Domain Does Not Restore Regulation to ΔR-N/C—Because a regulated CFTR trafficking response required the R domain, we asked whether its co-expression with ΔR-N/C would restore stimulation-dependent current and capacitance responses. This outcome would facilitate studies designed to identify a smaller region within the R domain that contributes to the ΔC_m. In baby hamster kidney cells, Chappe *et al.* (48) found that co-expression of the R domain with CFTR half-channels encoded by a bicistronic construct partially reduced the spontaneous anion efflux and channel activity of split ΔR-expressing cells and also partially restored their cAMP/PKA responsiveness. However, as seen in Fig. 6*A*, the co-expression of R domain cRNA with ΔR-N/C failed to significantly reduce its spontaneous current or restore cAMP/PKA regulation, despite a 5-fold excess of R domain cRNA. To ensure that the R domain polypeptide was expressed, Western blot analysis was performed using lysates from oocytes co-injected with R domain and ΔR-N/C cRNAs or with ΔR-N/C alone. The blot of Fig. 6*B* shows that the lack of recovery of regulated current was not because of a lack of R domain expression, but it likely results from an inability of the R domain to properly assemble with the half-channels in this system.

The NEG2 Region Is Required for cAMP/PKA-dependent CFTR Trafficking—The co-expression of R domain constructs with ΔR-N/C did not allow us to narrow the R region involved in regulated CFTR trafficking. Therefore, we progressively deleted amino acid segments from the C terminus of the 1–834 construct and co-expressed these with the complementary C-terminal construct, 835–1480. Of those examined (Table 1, part C), only the split CFTR combination 1–784 + 835–1480 generated significant currents above base-line levels. As illustrated in Fig. 7, *A* and *B*, this 51-amino acid deletion produced somewhat elevated basal currents while remaining responsive to cAMP/PKA stimulation. Unlike ΔR-N/C, 1–784 + 835–1480 CFTR retains 8 of 10 sites for cAMP/PKA-dependent channel gating (8). However, 1–784 + 835–1480 CFTR showed no stimulation-dependent increase in membrane capacitance (Fig. 7, *B* and *C*). Therefore, this combination of half-channels structurally dissociates the ΔC_m and ΔI_m responses of CFTR to cAMP/PKA stimulation. In addition, the data verify that the measured ΔC_m is not a technical artifact that is linked in some way to the ΔI_m. The absent C_m response suggests that 1–784 + 835–1480 CFTR lacks regulated recruitment to the plasma membrane and indicates that this region of the R domain accounts for the similar properties of ΔR-N/C.

Lying in the 784–835 region of the R domain is a stretch of negatively charged amino acids (amino acids 817–838) designated by Ma and co-workers (2, 49) as NEG2. In their prior studies, this region of the R domain influenced the gating properties of CFTR reconstituted into planar lipid bilayers. Its 22 amino acids have a net charge of −9, and the peptide exhibits significant α-helical content, assessed by CD spectroscopy (2). On this basis, we developed split CFTR constructs lacking the NEG2 region (1–816 + 839–1480), and we designated their co-expression as ΔNEG2 CFTR. As shown in Fig. 7*D*, their behavior was qualitatively similar to the larger deletion, 1–784 + 835–1480. As shown in Table 1, part C, the basal currents of

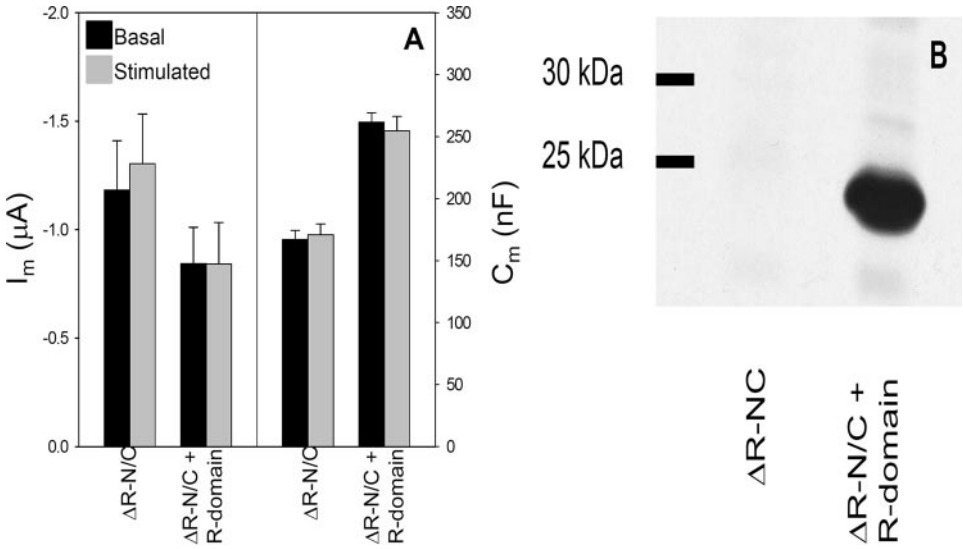

FIGURE 6. **Expression of the R domain does not induce regulated behavior of ΔR-N/C.** cRNA expression conditions are as follows: 0.5 ng each of ΔR-N/C cRNAs, with or without 5 ng of R domain, plus 1 ng of β_2-adrenergic receptor cRNA. *A,* mean basal and stimulated I_m and C_m values ΔR-N/C ($N = 3$; $n = 14$) and ΔR-N/C + R domain ($N = 3$; $n = 17$). The source of the difference in mean C_m values of these groups is not known; however, these values are within the range observed, and variation does arise from oocyte size and membrane folding (32). *B,* immunoblot of lysates from oocytes expressing ΔR-N/C or ΔR-N/C + R domain; expression conditions as in *A*. Membranes were probed with R domain-specific anti-CFTR monoclonal antibody (1:1000); see "Experimental Procedures" for protocol.

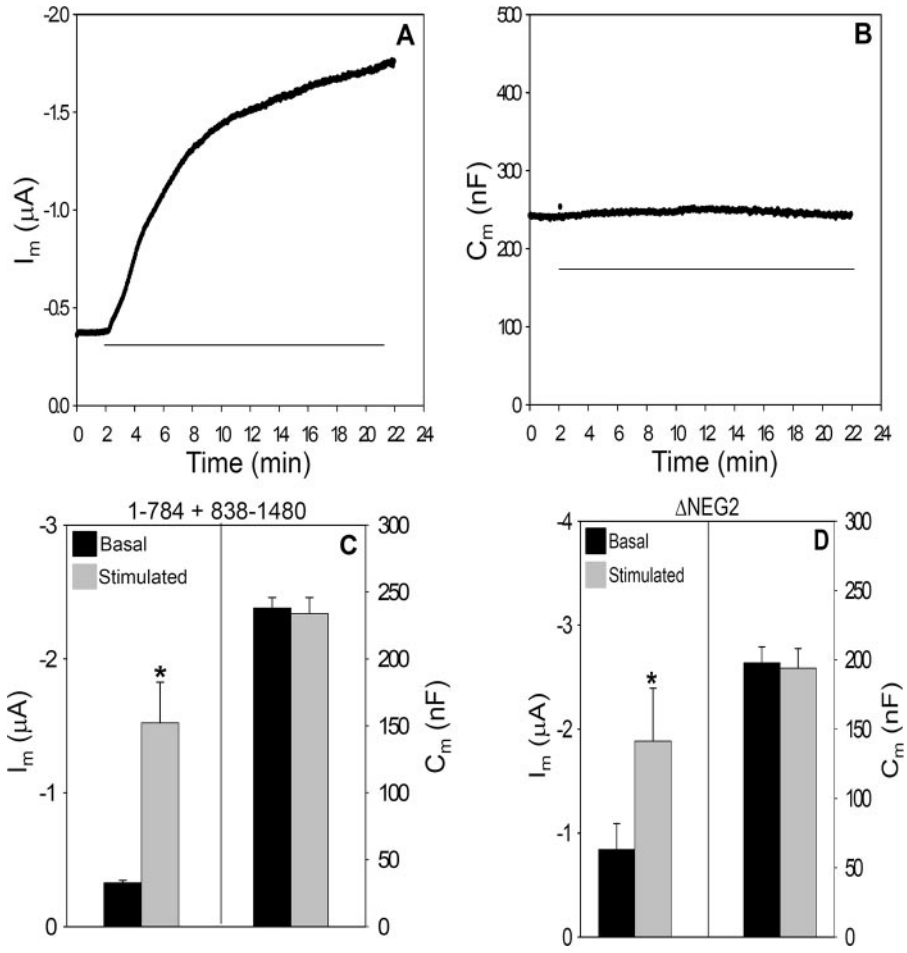

FIGURE 7. **Partial R domain deletions mimic the absence of a trafficking response in ΔR-N/C.** *A* and *B*, I_m and C_m recordings of split CFTR (1–784 + 835–1480) co-expressed with β_2-adrenergic receptor; all cRNAs are 1 ng/oocyte. *Horizontal line* indicates the addition of 10 μM isoproterenol. *C,* summary data for 1–784 + 835–1480 CFTR ($N = 3$; $n = 11$). *D,* summary data for split ΔNEG2 injected oocytes; cRNAs 1 ng/oocyte ($N = 4$; $n = 16$).

ΔNEG2 were more elevated, but the stimulated current levels were similar. As found for ΔR-N/C and 1–784 + 835–1480 CFTR, this channel did not display the cAMP/PKA-dependent stimulation of C_m that is characteristic of WT CFTR.

NEG2 Peptide Restores Agonist-activated ΔC_m—To determine whether the NEG2 peptide itself could influence the regulated trafficking of CFTR, we injected the peptide (residues 817–838) into oocytes expressing ΔNEG2. Based on prior experience with similar protocols (50), the 20-min period prior to initiation of stimulation should be more than sufficient for peptide diffusion within the oocyte. Fig. 8*A* provides the mean data from this set of experiments. Following NEG2 peptide injection, the basal and stimulated currents were not markedly different from those of ΔNEG2 alone; however, a significant ΔC_m response (29.2 ± 2.03 nF) to cAMP/PKA stimulation was now observed. Within this time frame, peptide injection was able to restore 65% of the ΔC_m response of WT CFTR. However, relative to the $\Delta I_m/\Delta C_m$ of WT CFTR (57 μA/nF), the ΔI_m of ΔNEG2-CFTR after peptide injection (1 μA) predicts a ΔC_m of 19 nF if the trafficking of ΔNEG2 contributes similarly to current as in WT CFTR. A change of 24 nF was observed, so that the return of regulated trafficking properties was not different from predicted.

To further assess the properties of NEG2, as done originally by Ma and co-workers (2), two additional peptides were synthesized that eliminated the helical content of NEG2 or reduced its net negative charge. One peptide (sNEG2) consists of a scrambled NEG2 sequence that disrupts the helical structure but preserves the negative charge; the other peptide, (hNEG2) has reduced negative charge (−9 to −3) but retains helical structure (2). The remaining negative charge of hNEG2 was necessary to maintain peptide solubility (2). As shown in Fig. 8*B*, the sNEG2 peptide did not restore the agonist-stimulated

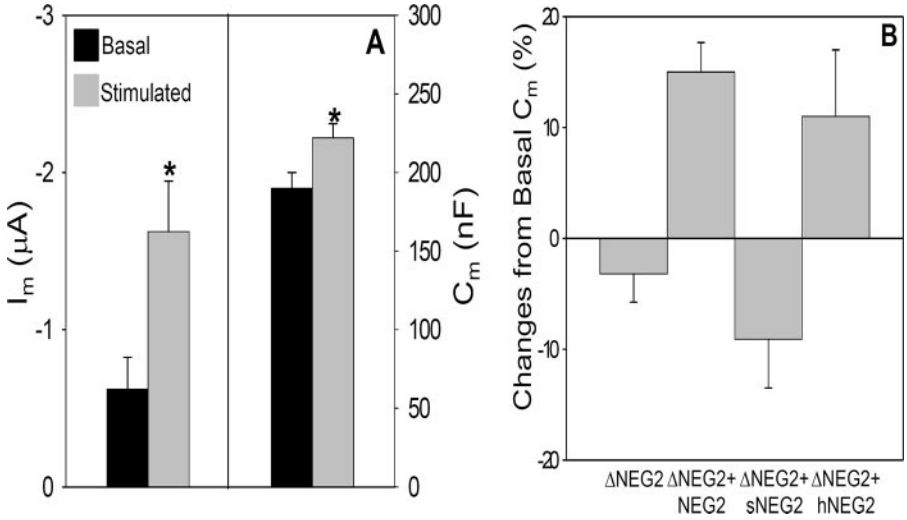

FIGURE 8. **Peptide injection restores regulated trafficking to ΔNEG2.** *A,* summary data for ΔNEG2 expressing oocytes injected with 23 nl of 50 mM NEG2 peptide (~1 nmol) prior to I_m and C_m recordings ($N = 4$; $n = 14$); cRNA is 7 ng/oocyte. *B,* summary data for changes in C_m (%) evoked by 10 μM isoproterenol following injection of the indicated peptide into oocytes expressing split ΔNEG2 CFTR (as in *A*). Sequences of peptides: NEG2, GLEISEEINEEDLKECFFDDME; sNEG2, LIKEFSEEDGECLMIDEDENEF; hNEG2, GLEISEQINQQNLKQSFFNDME. See Ref. 2 for discussion of peptide structures as determined by circular dichroism. sNEG2, $N = 3$ and $n = 12$; hNEG2, $N = 4$ and $n = 16$.

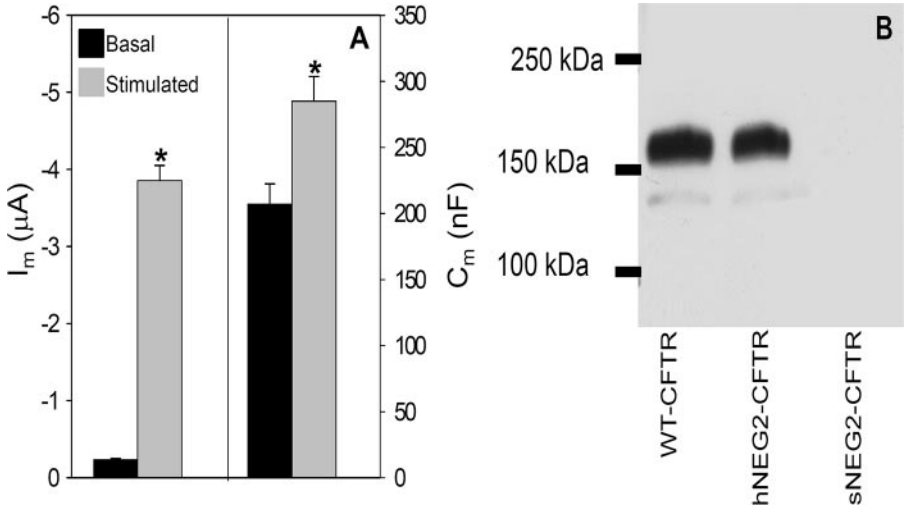

FIGURE 9. **hNEG2-CFTR retains regulated trafficking properties.** *A,* I_m and C_m summary data for hNEG2-CFTR ($N = 3$; $n = 13$). *B,* Western blot of HEK 293 cells transfected with WT CFTR, hNEG2-CFTR, or sNEG2-CFTR. Cells were transfected with 4 μg of cDNA for each construct; after 24 h, cells were harvested and subjected to immunoblot using monoclonal antibody directed against the CFTR C terminus (1:2500). Results are typical of three experiments.

increase in C_m, although hNEG2 peptide injection reproduced a similar ΔC_m response as that observed with native NEG2 peptide injection. Elimination of the agonist induced ΔC_m with sNEG2, and its preservation with hNEG2 suggests that the helical content of NEG2 is a primary requisite for this region to support the regulated trafficking of CFTR.

These findings were further explored by incorporating the sNEG and hNEG sequences into full-length CFTR. PCR-based mutagenesis (see "Experimental Procedures") was employed to generate these sequences within the NEG2 region. The resulting constructs were designated sNEG2-CFTR or hNEG2-CFTR. Similar to findings with hNEG2 peptide injection, hNEG2-CFTR yielded agonist induced increases in both I_m and C_m, as illustrated in Fig. 9*A*. In addition, the basal current of hNEG2-CFTR was similar to that observed for WT CFTR expression. In contrast, attempts to express sNEG2-CFTR did not yield currents higher than those observed in noninjected oocytes (data not shown). The explanation for this negative finding was provided by Western blots of HEK 293 cells transfected with WT CFTR, hNEG2-CFTR, or sNEG2-CFTR plasmids (Fig. 9*B*); WT and hNEG2-CFTR were expressed at similar levels, whereas the sNEG2-CFTR construct did not produce a detectable product. Nevertheless, treatment of sNEG2-CFTR-transfected HEK 293 cells with MG132 (5 μM, 16 h), to inhibit proteosome-mediated protein degradation, resulted in detection of immature sNEG2-CFTR by immunoblot (data not shown). This finding suggests that sNEG-CFTR is rapidly degraded, which would account for the absence of a functional current response. These data, in conjunction with the peptide co-injection experiments, strongly suggest that the NEG2 region is required for regulated CFTR trafficking and that its helical content is an important structural feature necessary for this response.

Syntaxin 1A Inhibition Is Eliminated in ΔR-N/C and ΔNEG2 CFTR—Prior studies have indicated that a physical interaction of syntaxin 1A (S1A) with the CFTR N terminus reduces the regulated currents of CFTR expressed in oocytes (51, 52). Other work (25) attributed the action of co-expressed S1A to an inhibition of CFTR trafficking, detected using membrane capacitance measurements and external epitope tag labeling, similar to the present studies. Given the requirement for the R domain and specifically the NEG2 region in regulated CFTR trafficking, we examined the influence of co-expressed S1A on the properties of ΔR-N/C and ΔNEG2 CFTR. As illustrated in Fig. 10, the action of S1A on WT CFTR recapitulated the results of prior studies in which its co-expression reduced cAMP/PKA-stimulated CFTR currents and eliminated the agonist-evoked ΔC_m. However, these inhibitory effects were absent when S1A was co-expressed with ΔR-N/C or ΔNEG2 CFTR. The elevated basal currents of ΔR-N/C and ΔNEG2 CFTR were not altered by S1A nor was the current response of ΔNEG2 CFTR to stimulation. Thus, these R domain deletion mutants, which exhibit no ΔC_m response to agonist, are also unresponsive to S1A inhibition. The functional interaction between this SNARE protein

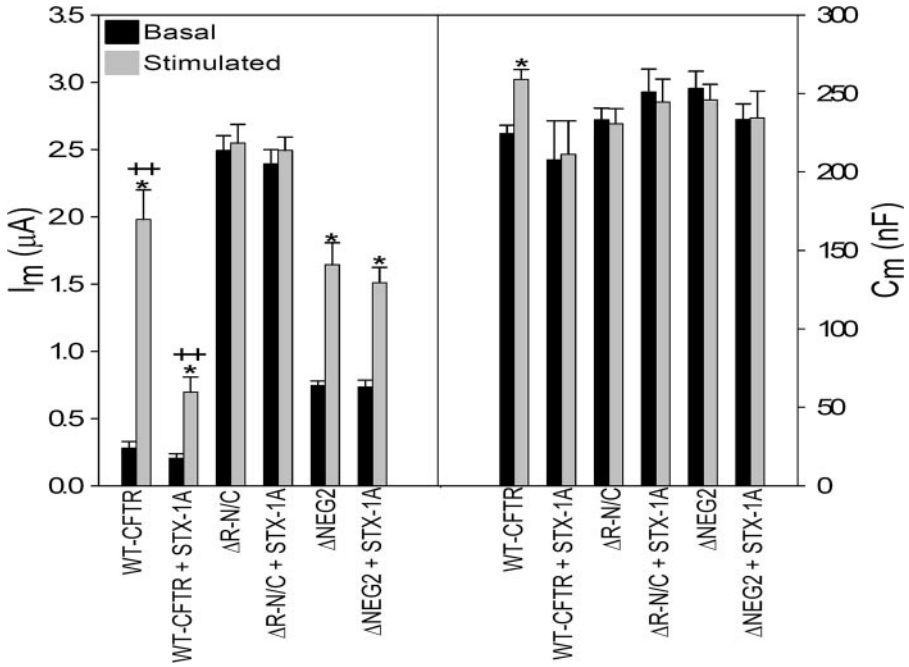

FIGURE 10. **Deletion of NEG2 region eliminates the effect of syntaxin 1A on CFTR-mediated ΔI_m and ΔC_m.** cRNA injections: WT-CFTR (1 ng), ΔR-N/C (1 ng total), or ΔNEG2 (7.5 ng) with or without S1A (10 ng), as indicated, plus β_2-adrenergic receptor (1 ng); stimulation with 10 μM isoproterenol. *, significant difference between basal and stimulated conditions ($p < 0.05$); ++ indicates a significant difference with S1A co-expression ($p < 0.05$). $N = 2$; $n = 9$, all groups.

and CFTR, like the regulated trafficking response of CFTR, requires the NEG2 region.

DISCUSSION

The primary goal in this work was to determine whether a structural feature, within CFTR itself, contributes to its cAMP/PKA-regulated trafficking at the plasma membrane. Our rationale was that the identification of a CFTR component that is required for the trafficking response could lead ultimately to elucidation of the trafficking mechanism, and potentially provide targets for modulating the apical membrane density of CFTR mutants (see Introduction).

Xenopus oocytes display a robust CFTR trafficking phenotype, and calculations based on the present data suggest that the recruitment of CFTR from intracellular compartments accounts for most of the current response in this system. Oocytes exhibit agonist-evoked, CFTR-dependent increases in membrane capacitance and in plasma membrane CFTR labeling using an expression construct containing a FLAG epitope tag in the fourth extracellular loop of CFTR, ECL4 (25). This approach has been used by others to measure the cell surface expression of ENaC (53, 54) and other channels (55). In the present studies, we confirmed this finding using a CFTR construct bearing an HA tag in ECL2, so-called EXT-CFTR. Gentzsch *et al.* (37) developed EXT-CFTR and characterized its regulated function using halide efflux measurements. As for WT CFTR, we observed increases in I_m and C_m from EXT-CFTR upon cAMP/PKA stimulation. The current/capacitance responses of WT and EXT-CFTR were similar (57 *versus* 67 pA/pF), indicating that its regulated plasma membrane trafficking properties replicate those of WT CFTR and CFTR tagged in ECL4. Thus, the detection of a stimulus-induced increase in plasma membrane CFTR is independent on the position or composition of the epitope tag.

cAMP/PKA-evoked changes in membrane capacitance were used to assess the trafficking of CFTR as its structural features were manipulated. Given that the initiation of both gating and trafficking responses require phosphorylation of the CFTR R domain, it was logical to begin this process using constructs in which the R domain was deleted. Csanady *et al.* (46) showed that gating properties of CFTR were maintained when split CFTR half-channels lacking the R domain were co-expressed in *Xenopus* oocytes, providing the opportunity to examine the relation of CFTR trafficking to R domain structure. As in prior studies (46), we found that split CFTR lacking the R domain, ΔR-N/C, exhibited spontaneous currents that were not significantly increased by cAMP/PKA stimulation. In addition, the agonist-induced ΔC_m, reflecting the regulated trafficking of WT CFTR to the cell surface, was eliminated, identifying the R domain as a necessary structural feature in this process.

R domainless and ΔNEG2 CFTRs exhibited a reduced functional half-life, resembling that of WT CFTR during continuous stimulation by cAMP/PKA. These findings suggested that under nonstimulated conditions, CFTR resides in an intracellular compartment where it is relatively stable. This stability may arise from the kinetics of plasma membrane trafficking steps that distribute CFTR predominantly to intracellular compartments in the absence of stimulation. As noted above, similar behavior is observed in response to the acute stimulation of GLUT4 and ENaC trafficking.

To further resolve the R region involved in stabilizing CFTR within the cell, segments of the R domain C terminus were progressively deleted from the half-channel construct that included the R domain (*e.g.* residues 1–834). Large R region deletions were problematic, however. As demonstrated previously (56, 57), functional CFTR expression was lost when regions at the N terminus of the R domain were eliminated. Nevertheless, the expression of constructs that eliminated smaller C-terminal segments of R revealed that removal of the NEG2 region eliminated agonist-stimulated trafficking of CFTR while retaining most of regulated conductance function of CFTR.

Confirming the importance of this segment, prior injection of NEG2 peptide restored a regulated trafficking response to ΔNEG2 CFTR, although the agonist-induced ΔC_m was reduced by ~35% compared with that of WT CFTR. The functional complementation of regulated CFTR trafficking by peptide injection depended on the previously determined helical struc-

ture of NEG2 (2), as peptide lacking helical content failed to recover agonist-evoked capacitance changes, despite the retention of negative charge. This feature was confirmed for full-length CFTR in which the NEG2 region was substituted by the helical counterpart, hNEG2. Nevertheless, hNEG2 retains a net negative charge of −3, which was minimally required for peptide solubility (2), and this may contribute to the regulated trafficking response observed.

The relatively short time for recovery of cAMP/PKA-regulated trafficking following NEG2 peptide injection (~30 min between injection and stimulation) suggests that the intracellular CFTR trafficking compartment that contributes to the increase in C_m with stimulation can be re-filled relatively quickly. Previous studies of CFTR turnover at the cell surface are compatible with this short time scale for recovery. For example, in T84 cells, ~50% of CFTR on cell surface was internalized within 15 min (23), and similar CFTR endocytic internalization rates were observed in COS-7 cells expressing WT CFTR (58). Time courses of CFTR internalization and recycling with similar kinetics were reported recently for polarized human airway cells (59). These findings suggest that CFTR endocytosis and recycling at the plasma membrane domain are sufficiently rapid to permit the formation of a trafficking compartment within the time frame of these experiments.

Evidence for the ability of the NEG2 peptide to functionally associate with NEG2-deleted CFTR was provided by Ma and co-workers (2). They showed that the addition of NEG2 to the cytoplasmic surface of WT or ΔNEG2-CFTR in lipid bilayers altered CFTR open probability in a biphasic, concentration-dependent manner. Because low NEG2 concentrations enhanced P_o, whereas higher NEG2 concentrations reduced CFTR P_o, Ma and co-workers (2) proposed that the amphipathic nature of the NEG2 helix facilitates its interaction with a gating inhibitory site in the nonphosphorylated channel, stabilizing the closed state, whereas its interaction with a stimulatory site in the phosphorylated channel augments channel opening. Overlaid on this concept, the present findings suggest that the NEG2 region interrupts the constitutive trafficking of CFTR to the plasma membrane when the channel is not phosphorylated, permitting its entry into a kinetically stable intracellular compartment. Subsequently, R domain phosphorylation would suppress these interactions of NEG2, which may include its association with components of the trafficking machinery, permitting the progression of phosphorylated CFTR to the surface membrane.

As a prototype for this model, we examined the influence of syntaxin 1A on the behavior of ΔR-N/C and ΔNEG2 CFTRs. The regulation of CFTR by this SNARE protein is complex, involving its physical interaction with the CFTR N-terminal tail, which itself influences channel open probability (60). In addition, prior work in oocytes showed that S1A co-expression with WT CFTR reduced its regulated trafficking to the cell surface (25), and this action was confirmed here by the inhibition of stimulated WT CFTR current and the block of agonist-induced ΔC_m associated with S1A co-expression (Fig. 10). As reported previously (25), we attribute this effect of S1A to its ability to retain CFTR within intracellular compartment(s), similar in principle to the concept that the NEG2 region is required for intracellular stabilization of CFTR under basal conditions. Thus, elimination of the NEG2 region allows CFTR to traffic constitutively to the plasma membrane, and this deletion also obviates the block of CFTR progression to the cell surface elicited by S1A expression. In this light, when CFTR is not phosphorylated, NEG2 may interact with a traffic regulatory protein, such as a SNARE protein, and this interaction causes intracellular CFTR retention within nonstimulated cells. It is possible also that this regulatory protein interaction is effected by another part of CFTR with which NEG2 associates. Nevertheless, attempts to further resolve the molecular details are outside the scope of this study.

In summary, cAMP/PKA stimulation increases cell surface expression of CFTR in addition to augmenting CFTR channel gating, and both modes of regulation require the R domain. Its removal permits CFTR gating in the absence of agonist stimulation and also eliminates the ability of the channel to enter a regulated trafficking pathway, resulting in the constitutive delivery of CFTR to the plasma membrane. Our findings identify the NEG2 region of the R domain, amino acids 817–838, as the critical structural element of CFTR that is required for its phosphorylation-dependent trafficking. Accordingly, the intracellular retention of CFTR under nonphosphorylated conditions may involve interactions of the NEG2 region with proteins that mediate regulated membrane trafficking events. Because NEG2 also influences channel gating (2), these findings imply that regulation of the gating and trafficking functions of CFTR are structurally linked. The identification of NEG2 as a required structural component should lead to a better understanding of CFTR trafficking mechanisms, including the associated protein-protein interactions.

Acknowledgments—We thank Dr. Daniel C. Devor for advice and discussions in the course of these studies. We also thank Drs. Fei Sun, Hui Zhang, Steven Condliffe, and Michael Butterworth for their assistance with various aspects of this work.

REFERENCES

1. Bertrand, C. A., and Frizzell, R. A. (2003) *Am. J. Physiol.* **285,** C1–C18
2. Xie, J., Adams, L. M., Zhao, J., Gerken, T. A., Davis, P. B., and Ma, J. (2002) *J. Biol. Chem.* **277,** 23019–23027
3. Chambers, L., Rollins, B., and Tarran, R. (2007) *Respir. Physiol. Neurobiol.* **159,** 256–270
4. Pilewski, J., and Frizzell, R. (1999) *Physiol. Rev.* **79,** S215–S255
5. Riordan, J. R., Rommens, J. M., Kerem, B., Alon, N., Rozmahel, R., Grzelczak, Z., Zielenski, J., Lok, S., Plavsic, N., Chou, J. L., *et al.* (1989) *Science* **245,** 1066–1073
6. Higgins, C. F. (1992) *Annu. Rev. Cell Biol.* **8,** 67–113
7. Gadsby, D. C., and Nairn, A. C. (1999) *Physiol. Rev.* **79,** S77–S107
8. Chang, X. B., Tabcharani, J. A., Hou, Y. X., Jensen, T. J., Kartner, N., Alon, N., Hanrahan, J. W., and Riordan, J. R. (1993) *J. Biol. Chem.* **268,** 11304–11311
9. Ostedgaard, L. S., Baldursson, O., Vermeer, D. W., Welsh, M. J., and Robertson, A. D. (2000) *Proc. Natl. Acad. Sci. U. S. A.* **97,** 5657–5662
10. Baker, J. M., Hudson, R. P., Kanelis, V., Choy, W. Y., Thibodeau, P. H., Thomas, P. J., and Forman-Kay, J. D. (2007) *Nat. Struct. Mol. Biol.* **14,** 738–745
11. Anderson, M. P., Berger, H. A., Rich, D. P., Gregory, R. J., Smith, A. E., and Welsh, M. J. (1991) *Cell* **67,** 775–784
12. Cheng, S. H., Rich, D. P., Marshall, J., Gregory, R. J., Welsh, M. J., and Smith, A. E. (1991) *Cell* **66,** 1027–1036
13. Tabcharani, J. A., Chang, X. B., Riordan, J. R., and Hanrahan, J. W. (1991)

Nature **352,** 628–631
14. Vergani, P., Lockless, S. W., Nairn, A. C., and Gadsby, D. C. (2005) *Nature* **433,** 876–880
15. Smith, P. C., Karpowich, N., Millen, L., Moody, J. E., Rosen, J., Thomas, P. J., and Hunt, J. F. (2002) *Mol. Cell* **10,** 139–149
16. Luo, J., Pato, M. D., Riordan, J. R., and Hanrahan, J. W. (1998) *Am. J. Physiol.* **274,** C1397–C1410
17. Ma, J., Zhao, J., Drumm, M. L., Xie, J., and Davis, P. B. (1997) *J. Biol. Chem.* **272,** 28133–28141
18. Winter, M. C., and Welsh, M. J. (1997) *Nature* **389,** 294–296
19. Baldursson, O., Ostedgaard, L. S., Rokhlina, T., Cotten, J. F., and Welsh, M. J. (2001) *J. Biol. Chem.* **276,** 1904–1910
20. Bradbury, N. A., Jilling, T., Berta, G., Sorscher, E. J., Bridges, R. J., and Kirk, K. L. (1992) *Science* **256,** 530–532
21. Schwiebert, E. M., Gesek, F., Ercolani, L., Wjasow, C., Gruenert, D. C., Karlson, K., and Stanton, B. A. (1994) *Am. J. Physiol.* **267,** C272–C281
22. Lukacs, G. L., Segal, G., Kartner, N., Grinstein, S., and Zhang, F. (1997) *Biochem. J.* **328,** 353–361
23. Prince, L. S., Workman, R. B., Jr., and Marchase, R. B. (1994) *Proc. Natl. Acad. Sci. U. S. A.* **91,** 5192–5196
24. Takahashi, A., Watkins, S. C., Howard, M., and Frizzell, R. A. (1996) *Am. J. Physiol.* **271,** C1887–C1894
25. Peters, K. W., Qi, J., Watkins, S. C., and Frizzell, R. A. (1999) *Am. J. Physiol.* **277,** C174–C180
26. Ameen, N. A., Marino, C., and Salas, P. J. (2003) *Am. J. Physiol.* **284,** C429–C438
27. Lehrich, R. W., Aller, S. G., Webster, P., Marino, C. R., and Forrest, J. N., Jr. (1998) *J. Clin. Investig.* **101,** 737–745
28. Lukacs, G. L., Chang, X. B., Bear, C., Kartner, N., Mohamed, A., Riordan, J. R., and Grinstein, S. (1993) *J. Biol. Chem.* **268,** 21592–21598
29. Silvis, M. R., Picciano, J. A., Bertrand, C., Weixel, K., Bridges, R. J., and Bradbury, N. A. (2003) *J. Biol. Chem.* **278,** 11554–11560
30. Heda, G. D., Tanwani, M., and Marino, C. R. (2001) *Am. J. Physiol.* **280,** C166–C174
31. Sharma, M., Benharouga, M., Hu, W., and Lukacs, G. L. (2001) *J. Biol. Chem.* **276,** 8942–8950
32. Weber, W. M., Cuppens, H., Cassiman, J. J., Clauss, W., and Van Driessche, W. (1999) *Pfluegers Arch.* **438,** 561–569
33. Schillers, H., Danker, T., Madeja, M., and Oberleithner, H. (2001) *J. Membr. Biol.* **180,** 205–212
34. Cunningham, S. A., Worrell, R. T., Benos, D. J., and Frizzell, R. A. (1992) *Am. J. Physiol.* **262,** C783–C788
35. Lang, J., Fukuda, M., Zhang, H., Mikoshiba, K., and Wollheim, C. B. (1997) *EMBO J.* **16,** 5837–5846
36. Goldin, A. L. (1991) *Methods Cell Biol.* **36,** 487–510
37. Gentzsch, M., Chang, X. B., Cui, L., Wu, Y., Ozols, V. V., Choudhury, A., Pagano, R. E., and Riordan, J. R. (2004) *Mol. Biol. Cell* **15,** 2684–2696
38. Liu, X., Smith, S. S., Sun, F., and Dawson, D. C. (2001) *J. Gen. Physiol.* **118,** 433–446
39. Uezono, Y., Bradley, J., Min, C., McCarty, N. A., Quick, M., Riordan, J. R., Chavkin, C., Zinn, K., Lester, H. A., and Davidson, N. (1993) *Receptors Channels* **1,** 233–241
40. Schultz, B. D., Frizzell, R. A., and Bridges, R. J. (1999) *J. Membr. Biol.* **170,** 51–66
41. Jones, H. M., Hamilton, K. L., Papworth, G. D., Syme, C. A., Watkins, S. C., Bradbury, N. A., and Devor, D. C. (2004) *J. Biol. Chem.* **279,** 15531–15540
42. Ma, D., Zerangue, N., Raab-Graham, K., Fried, S. R., Jan, Y. N., and Jan, L. Y. (2002) *Neuron* **33,** 715–729
43. Butterworth, M. B., Edinger, R. S., Johnson, J. P., and Frizzell, R. A. (2005) *J. Gen. Physiol.* **125,** 81–101
44. Sargeant, R. J., and Paquet, M. R. (1993) *Biochem. J.* **290,** 913–919
45. Shimkets, R. A., Lifton, R. P., and Canessa, C. M. (1997) *J. Biol. Chem.* **272,** 25537–25541
46. Csanady, L., Chan, K. W., Seto-Young, D., Kopsco, D. C., Nairn, A. C., and Gadsby, D. C. (2000) *J. Gen. Physiol.* **116,** 477–500
47. Devidas, S., Yue, H., and Guggino, W. B. (1998) *J. Biol. Chem.* **273,** 29373–29380
48. Chappe, V., Irvine, T., Liao, J., Evagelidis, A., and Hanrahan, J. W. (2005) *EMBO J.* **24,** 2730–2740
49. Ma, J. (2000) *News Physiol. Sci.* **15,** 154–158
50. Condliffe, S. B., Zhang, H., and Frizzell, R. A. (2004) *J. Biol. Chem.* **279,** 10085–10092
51. Naren, A., Nelson, D., Xie, W., Jovov, B., Pevsner, J., Bennett, M., Benos, D., Quick, M., and Kirk, K. (1997) *Nature* **390,** 302–305
52. Naren, A. P., Quick, M. W., Collawn, J. F., Nelson, D. J., and Kirk, K. L. (1998) *Proc. Natl. Acad. Sci. U. S. A.* **95,** 10972–10977
53. Condliffe, S. B., Carattino, M. D., Frizzell, R. A., and Zhang, H. (2003) *J. Biol. Chem.* **278,** 12796–12804
54. Firsov, D., Robert-Nicoud, M., Gruender, S., Schild, L., and Rossier, B. C. (1999) *J. Biol. Chem.* **274,** 2743–2749
55. Dubel, S. J., Altier, C., Chaumont, S., Lory, P., Bourinet, E., and Nargeot, J. (2004) *J. Biol. Chem.* **279,** 29263–29269
56. Rich, D. P., Gregory, R. J., Anderson, M. P., Manavalan, P., Smith, A. E., and Welsh, M. J. (1991) *Science* **253,** 205–207
57. Rich, D. P., Gregory, R. J., Cheng, S. H., Smith, A. E., and Welsh, M. J. (1993) *Receptors Channels* **1,** 221–232
58. Prince, L. S., Peter, K., Hatton, S. R., Zaliauskiene, L., Cotlin, L. F., Clancy, J. P., Marchase, R. B., and Collawn, J. F. (1999) *J. Biol. Chem.* **274,** 3602–3609
59. Swiatecka-Urban, A., Brown, A., Moreau-Marquis, S., Renuka, J., Coutermarsh, B., Barnaby, R., Karlson, K. H., Flotte, T. R., Fukuda, M., Langford, G. M., and Stanton, B. A. (2005) *J. Biol. Chem.* **280,** 36762–36772
60. Naren, A., Cormet-Boyaka, E., Fu, J., Villain, M., Blalock, J., Quick, M., and Kirk, K. (1999) *Science* **286,** 544–548